MODELING AND SIMULATION OF
LIMESTONE CALCINATION IN ROTARY KILNS

Marcio A. Martins, aredes@demec.ufmg.br
Leandro S. Oliveira, leandro@deq.ufmg.br
Adriana S. Franca, franca@deq.ufmg.br
Chemical Engineering Department/Universidade Federal de Minas Gerais
R. Espirito Santo, 35 – 6° andar 30160-030 Belo Horizonte, MG, Brazil

Abstract. A one-dimensional mathematical model was developed for the simulation of limestone calcination in rotary kilns. The model is comprised of ordinary differential equations derived from mass and energy conservation principles. The system of equations is solved by a fourth-order Runge-Kutta method. The model predicts, in the axial direction, temperature profiles for the bed of particles, the gas phase and the kiln internal wall. It also predicts the composition profile for the bed. The results from the simulation of the calcination systems presented good agreement with experimental data measured in a pilot kiln.

*Keywords***:** lime, heat transfer, numerical analysis.

1. INTRODUCTION

Mathematical models have been developed in the past decades to describe calcination processes in rotary kilns (Gordon, 1969; Sood *et al.*, 1972; Li & Friday, 1974; Brooks, 1989; Perron *et al.*, 1992; Davis, 1996). The models were usually built upon the basic principles of conservation of heat and mass, and took into account chemical reactions. No models were found in the literature for the calcination of limestone in rotary kilns to produce lime. The objective of this work was to modify the model proposed by Perron *et al.* (1992) for petroleum coke calcination in order to describe calcination of limestone in rotary kilns. Modifications were introduced to the sub-models to account for variations in the model parameters and thermophysical properties as a function of the state variables. Also, some of the sub-models were replaced by more suitable ones.

2. MATHEMATICAL MODELLING

Limestone calcination in rotary kilns will be described by means of a model based on mass and energy conservation. Heat transfer by conduction, convection and radiation is taken into account. Mass transfer occuring between the solid and gas phases is mainly due to natural gas combustion reactions and release of CO_2 from the thermal decomposition of the limestone in the bed. Figure 1 presents the control volumes used to develop the model, representing the kiln cross section with respect to the axial (x) direction.
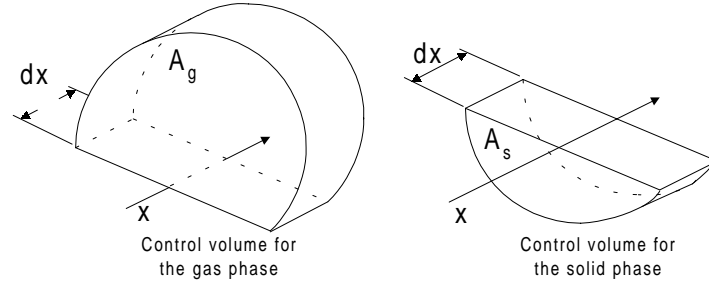
Figure 1 – Control volumes for the gas and the solid phases.

The differential control volumes (Fig.1) are defined as $dV_g = A_g\,dx$ for the gas phase and $dV_s = A_s\,dx$ for the solid phase. Each dependent variable is represented by an average in the x direction, for each control volume.

Assuming steady state conditions, the mass conservation equations can be written as

$$\frac{d}{dx}\left(u_s.A_s.\rho_i\right)= m_i + R_i$$

$$\frac{d}{dx}\left(u_g.A_g.\rho_i\right)= m_i + R_i$$

(1)

where u_s and u_g are the velocities of the solid and the gas phase (m·s⁻¹), respectively, A_s and A_g are the cross-sectional areas of the solid and the gas phases (m²), respectively, ρ_i is the density of species i (kg·m⁻³), m_i is the mass flow rate of species i per unit length of kiln (kg·m⁻¹·s⁻¹) and R_i is the rate of consumption of species i (kg·m⁻¹·s⁻¹). The energy equations were developed assuming negligible viscous dissipation and that the variations in kinetic and potential energy are not significant (Perron *et al.*, 1992):

$$G_s\,Cp_s\,\frac{dT_s}{dx} = \sum_{i=1}^{m}Q_i + \sum_{j=1}^{n}H_j m_j + \sum_{k=1}^{o}\Delta H_k R_k$$

$$G_g\,Cp_g\,\frac{dT_g}{dx} = \sum_{i=1}^{m}Q_i + \sum_{j=1}^{n}H_j m_j + \sum_{k=1}^{o}\Delta H_k R_k$$

(2)

where G_g and G_s are the mass flowrates of the gas and the solid phases (kg·s⁻¹), respectively, Cp_g and Cp_s are the heat capacities of the gas and the solid phases (kJ·kg⁻¹·K⁻¹), respectively, T_g and T_s are the temperatures of the gas and the solid phases (K), respectively, Q_i is heat flowrate per unit length by the radiation, the conduction and the convection (kJ·m⁻¹·s⁻¹), H_i is the sensible heat due to the mass transfer of species j, between the phases (kJ·kg⁻¹), ΔH_k is the heat of the reaction k (kJ·kg⁻¹) and R_k is the the rate of consumption per unit of length of species i due to the reaction k (kJ·m⁻¹·s⁻¹).

The sub-models related to the terms in Eqs. 1 and 2 are described as follows.

2.1 Solid transport equations

Modelling solids flow in a rotary kiln is quite complex, since physical, chemical and rheological properties vary along the bed. The major factors affecting bed motion in the axial direction are bed height variation, particles fluidization due to flow of volatile components

released from the bed, and properties dependence on temperature. There is an extensive amount of work on solids flow in rotary kilns and the model presented here for bed axial velocity (u_s) is based on the studies developed by Perron & Bui (1990):

$$u_s = K \frac{vr^2}{h^2 \cos(\phi) + \left(2h\sqrt{2hr - h^2}\right)\sin(\phi)}$$

(3)

where K is a characteristic constant, v is the kiln inclination angle (rad), r is the kiln internal radius (m), ϕ is the dynamic angle of repose (rad) and h is the bed height (m).

2.2 Heat transfer equations

Heat fluxes are calculated using empirical correlations, specific for rotary kilns. Heat transfer by radiation between the gas phase and the bed and between the gas phase and the kiln internal wall can be evaluated by the equations developed by Hottel & Sarofim (1967), valid for $\varepsilon \geq 0.8$:

$$Q_{rgk} = \sigma A_{rgk}\left(\varepsilon_k + 1\right)\left(\frac{\varepsilon_g T_g^4 - \alpha_g T_k^4}{2}\right) \qquad k = s, w$$

(4)

where Q_{rgk} is the radiative heat flux per unit length of kiln, between the gas and the solid phases, and the gas and the internal wall (kJ·m^{-1}·s^{-1}), σ is Stefan-Boltzmann constant (5,67×10^{-8} J·m^{-2}·K^{-4}·s^{-1}), A_{rgk} is the area of heat transfer per unit length of kiln (m), ε and α are the emissivity and absorptivity.

Heat fluxes by convection between the gas phase and the bed and between the gas phase and the kiln internal wall are evaluated as

$$Q_{cgk} = h_{cgk} A_{cgk}\left(T_g - T_k\right) \qquad k = s, w$$

(5)

where Q_{cgk} is the convective heat flux per unit length of kiln, between the gas and the solid phases, and the gas phase and the internal wall (kJ·m^{-1}·s^{-1}), A_{cgk} is the area of heat transfer per unit length of kiln (m), and h_{cgk} are the heat transfer coefficients given by (Tscheng & Watkinson, 1979)

$$h_{cgs} = 0.46 \frac{k_g}{D_e} Re_D^{0.535} Re_\omega^{0.104} \eta^{-0.341} \quad \text{and} \quad h_{cgw} = 1.54 \frac{k_g}{D_e} Re_D^{0.575} Re_\omega^{-0.292}$$

(6)

where D_e is the hydraulic diameter (m), Re_D and Re_ω are the axial and the angular Reynolds numbers, k_g is the thermal conductivity of the gas phase (kJ·m^{-1}·K^{-1}·s^{-1}) and η is the degree of fill of the kiln. The hydraulic diameter D_e, Re_D and Re_ω are evaluated as follows

$$D_e = 4\frac{A_g}{A_{cgs} + A_{cws}}, \quad Re_D = \frac{\rho_g u_g D_e}{\mu_g}, \quad Re_\omega = \frac{\rho_g \omega D_e^2}{\mu_g}$$

(7)

Heat flux by radiation between the coke bed and the kiln internal wall is evaluated according to the relationship given by Ketlakh & Tsibin (1978):

$$Q_{rws} = \sigma \, A_{rws} \, \varepsilon_w \, \varepsilon_s \, (1 - \varepsilon_g) \, \Omega \left(T_w^4 - T_s^4 \right) \tag{8}$$

where Q_{rws} is the radiative heat flux per unit length of kiln, between the solid phase and the internal wall ($kJ \cdot m^{-1} \cdot s^{-1}$), A_{rws} is the area of heat transfer per unit length of kiln (m), and Ω is form factor based on the internal wall and the bed.

Heat transfer by conduction between the coke bed and the kiln internal wall is given by

$$Q_{cws} = h_{cws} \, A_{cws} (T_w - T_s) \tag{9}$$

where Q_{cws} is the conductive heat flux per unit length of kiln, between the solid phase and the internal wall ($kJ \cdot m^{-1} \cdot s^{-1}$), A_{cws} is the area of heat transfer per unit length of kiln (m), with the heat transfer coeficient (h_{cws}) evaluated using the empirical correlation developed by Tscheng & Watkinson (1979):

$$h_{cws} = 11.6 \frac{k_b}{A_{cws}} \left(\frac{\omega R_i^2 \Gamma}{\alpha_b} \right)^{0.3} \tag{10}$$

where k_b is the thermal conductivity of the bed ($kJ \cdot m^{-1} \cdot K^{-1} \cdot s^{-1}$), A_{cws} is the heat transfer area per unit length of kiln (m), ω is the kiln rotational speed ($rad \cdot s^{-1}$), Γ is the angle of fill of kiln (rad). The heat consumption rate during limestone calcination can be evaluated as $Q_r = R\Delta H$.

The temperature at the kiln internal wall is evaluated by solving the equations that describe heat transfer through the wall. Heat fluxes due to convection, conduction and radiation penetrate the internal wall comprised of refractory bricks. The heat is transmitted in the radial direction, through the wall's refractory and steel layers. The heat is then released at the kiln external wall. A schematic representation of the heat fluxes is presented in Fig. 2.
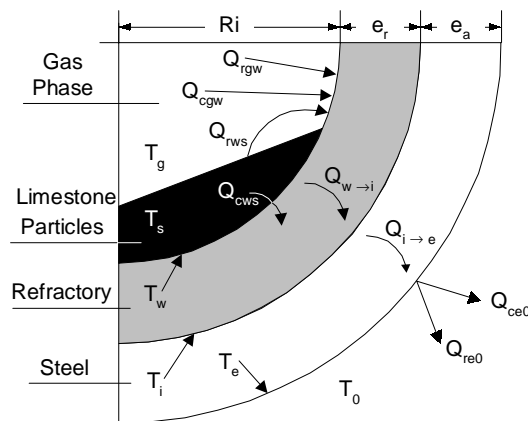

Figure 2 – Schematic representation of the heat fluxes in rotary kiln.

The heat flux by conduction in the angular direction (regenerative flux) was considered negligible (Barr *et al.*, 1989). An energy balance in radial direction leads to the following equations:

$$Q_{rws} + Q_{cws} + Q_{rgw} + Q_{cgw} = Q_{w \rightarrow i} \tag{11}$$

$$Q_{w \to i} = Q_{i \to e} \tag{12}$$

$$Q_{i \to e} = Q_{ce0} + Q_{re0} \tag{13}$$

Heat fluxes due to conduction are evaluated as (Pitts & Sissom, 1991)

$$Q_{w \to i} = \frac{2\pi}{k_r \ln\left[(R_i + e_r)/R_i\right]}(T_w - T_i) \tag{14}$$

$$Q_{i \to e} = \frac{2\pi}{k_a \ln\left[(R_i + e_r + e_a)/(R_i + e_r)\right]}(T_i - T_e) \tag{15}$$

The heat losses due to radiation and convection at the kiln external wall are given by (Özisik, 1985):

$$Q_{re0} = \sigma A_e \varepsilon_e \left(T_e^4 - T_0^4\right) \tag{16}$$

$$Q_{ce0} = h_{ce0} A_e \left(T_e - T_0\right) \tag{17}$$

Heat tranfer by convection between the kiln external wall and the surroundings can be forced or natural. In the case of forced convection ($Re_D^2 > Gr_D$), the heat transfer coefficient is evaluated as (Özisik, 1985)

$$Nu_m = h_{ce0}\frac{D}{k_0} = 0.3 + \frac{0.62\,Re^{1/2}\,Pr^{1/3}}{\left[1 + \left(\frac{0,4}{Pr}\right)^{2/3}\right]^{1/4}}\left[1 + \left(\frac{Re}{28200}\right)^a\right]^b$$

$$\begin{array}{ll} a = 5/8;\ b = 4/5 & 10^2 < Re_D < 2 \times 10^4 \\ a = 1/2;\ b = 1 & 4 \times 10^4 < Re_D < 10^7 \end{array} \tag{18}$$

where

$$Re_D = \frac{\rho D u_\infty}{\mu}, \quad Gr_D = \frac{gD^3}{v^2}\frac{|\rho - \rho_D|}{\rho}, \quad Pr = \frac{\mu Cp}{k_0} \tag{19}$$

where Nu_m is the average Nusselt number, Gr_D is Grashoff number for the gas phase.

For natural convection ($Re_D^2 < Gr_D$), the heat transfer coefficient is evaluated as (Özisik, 1985):

$$Nu_m = h_{ce0}\frac{D}{k_0} = 0.6 + \frac{0.386\,(Gr_D\,Pr)^{1/6}}{\left[1 + \left(\frac{0.559}{Pr}\right)^{9/16}\right]^{8/27}} \qquad 10^{-4} < Gr_D Pr < 10^{12} \tag{20}$$

In order to evaluate the the kiln internal wall temperature (T_w), the temperature at the steel/refractory interface (T_i) and the kiln external wall temperature (T_e), Eqs. 4, 5, 8, 9 and 14 are applied to Eq. 11, Eqs. 14 and 15 are applied to Eq. 12, and Eqs. 15, 16 and 17 are applied to Eq. 13, generating a system of nonlinear equations. This system of equations is solved by the Picard iteration scheme coupled to a relaxation formula (Reddy & Gartling, 1994), with T_w^4 e T_e^4 approximated by

$$T_w^4 = T_{w,n} \left(T_{w,n-1}^3 \right) \quad \text{and} \quad T_e^4 = T_{e,n} \left(T_{e,n-1}^3 \right) \tag{21}$$

where the subscripts n and n-1 correspond to the present and previous iterations, respectively. This results in a linearization procedure, since temperature values at the previous iterations are known.

2.3 Mass transfer equations

The mathematical models available in the literature for the limestone calcination rate are based on different types of assumptions and present different levels of complexity. In all the relevant works, the kinetics models were developed for a single limestone particle and took into account its interaction with the gas phase. In the present work, the model presented by Hills (1968) was adopted due to the fact that it is applicable to particle diameters up to 23mm. It also explicitly takes into account the effects of the system equilibrium pressure, the CO_2 partial pressure and gas velocity over the particles on the thermal decomposition rate. The particles thermal decomposition is treated as a moving boundary problem. The equation for the decomposition of a limestone composed of 98% of calcium carbonate is

$$CaCO_3 \quad \rightarrow \quad CaO \quad + \quad CO_2 \quad - \quad \Delta Hc \tag{22}$$

where ΔH_c is the reaction heat (4×10^4 J/mol). The equations for the thermal decomposition specific rate of limestone used in this work are exactly as presented by Hills (1968).

According to Watkinson & Brimacombe (1982), the limestone bed can be described as a rolling bed. The rolling bed is comprised of a rolling and a stationary layer. In the rolling layer, the particles are mixed to the gas phase, whereas in the stationary layer they are not. Martins & Oliveira (1998) presented a set of equations to evaluate the petroleum coke bed calcination rate as a function of the specific combustion rate of the particles and their residence time in each layer of the rolling bed. These equations can be used to evaluate the thermal decomposition rate of limestone if the specific combustion rate is replaced by the specific decomposition rate (R_{sc}).

3. IMPLEMENTATION

The model for the limestone calcination kiln is comprised of 4 ordinary differential equations, corresponding to the mass and energy conservation equations 1 and 2, and a large set of nonlinear algebraic equations. The dependent variables are calcium carbonate mass fraction in the solid bed, carbon dioxide mass fraction in the gas phase, and solid and gas temperatures. The system of equations must be solved iteratively. A fourth-order Runge-Kutta method was employed for the solution of the differential equations. The rotary kiln for limestone calcination modeled and simulated in the present work is equivalent to that described by Henein *et al.* (1983). The kiln design data are presented in Table 1. The kiln operational variables used in the simulation runs (Watkinson & Brimacombe, 1982) are presented in Table 2. The feed composition was considered to be 98.6% calcium carbonate.

Table 1. Design data for the limestone calcination kiln

Geometric parameters	Value	Unit
Length	5.5	m
Internal radius	0.203	m
External radius	0.305	m
Inclination	1.07	deg
Refractory thickness	0.092	m
Shell thickness	0.010	m

Table 2. Operational variables of the limestone calcination kiln

Operational variables	Value	Unit
Limestone feed rate	47.6/61.7	kg/h
Primary air rate	127.3	kg/h
Natural gas rate	7.29	kg/h
System total pressure	1	atm
Kiln rotational speed	1.5	rpm
Limestone feed temperature	245	^{o}C
Primary air temperature	25	^{o}C
Natural gas feed temperature	25	^{o}C

4. RESULTS AND DISCUSSION

For the numeric solution of the heat and mass transfer equations 100 integration points were used, distributed evenly in the axial length of the kiln. The effect of the number of integration points (np) in the convergence of the solution was made in a previous work (Martins, 1999). The discreet values of 50, 100, 200, 450 and 900 integration points were tested and the convergence of the solution was verified except for np=50. Through that analysis it was verified that np=100 is appropriate for this work. The simulation results for the limestone bed, gas phase and kiln internal wall temperature profiles are presented in Figs. 3 and 4 respectively, where they are compared to the experimental measurements obtained by Watkinson & Brimacombe (1982).

The temperature data were measured by thermocouples inserted throughout the kiln. In Figure 3a, it is clearly seen that, from the limestone feed position (0m) up to 3.5m in the kiln, the increase in temperature is solely due to heating of the bed. At approximately 3.5m, calcination of the bed begins for a limestone feed rate of 47.6 kg/h. Temperature remains nearly constant due to the endothermicity of the calcination reaction. Notice that for a feed rate of 61.7 kg/h the onset of calcination is delayed due to the fact that a larger amount of mass needs more time to heat up to reaction temperatures. The rapid increase in temperature at the end of the kiln indicates that most of the bed have already been calcined before that portion of the kiln. The predicted temperature profiles for the bed presented good agreement with experimental data by Watkinson & Brimacombe (1982).

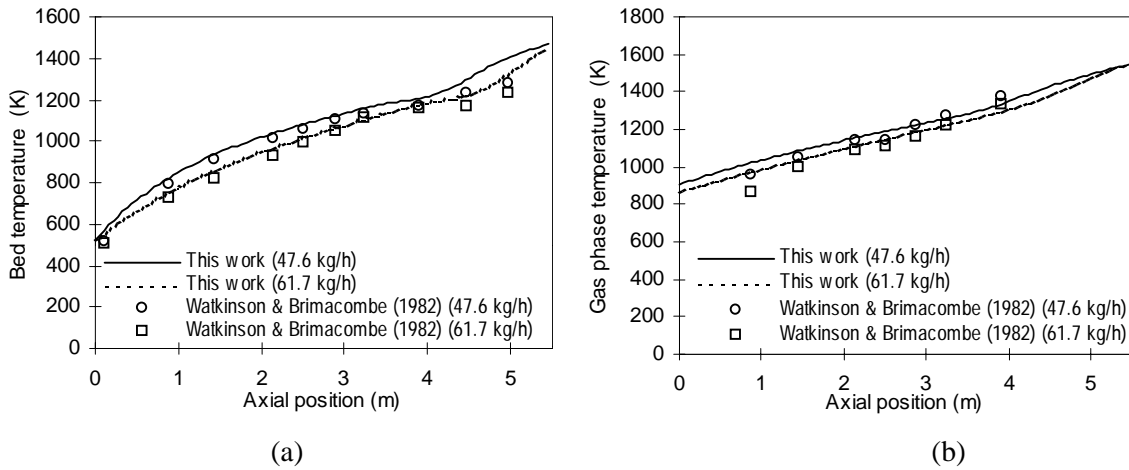(a)   (b)

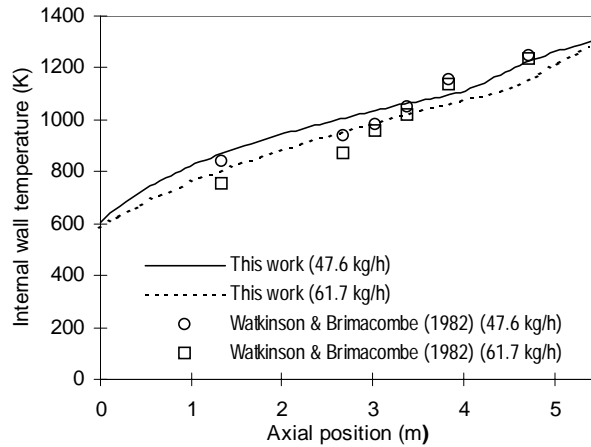Figure 3 – Temperature profile (a) limestone bed and (b) gas phase.

Figure 4 – Internal wall temperature profile.

The predicted temperature for the gas phase (Fig. 3b) decreases in a nearly linear fashion from the gas feed end (5.5m) to its exit end of the kiln (0m) for both limestone feed rates used in the simulation runs. The predicted results also agreed well with the experimental data. The predicted temperature profiles for the kiln internal wall (Fig 4) presented similar behavior to the measured data. In the experimental work by Watkinson & Brimacombe (1982) the thermocouples were embedded at 12.7mm within the refractory bricks, and the predicted values were calculated in this same position. Once the temperatures of the internal wall and the refractory-stell junction were already calculated, the temperature at 12.7mm within the refractory shell was calculated by eq. 14.

Watkinson & Brimacombe (1982) took samples from the kiln during calcination, at positions between 2 and 5.5m, for the experiments with limestone feed rate of 47.6 kg/h. These samples were analyzed and for each of the samples the percentage conversion of $CaCO_3$ to CaO (percentage calcination) was calculated. Figure 5 presents the curve for the calculated percentage calcination as a function of the bed temperature utilizing the proposed model.
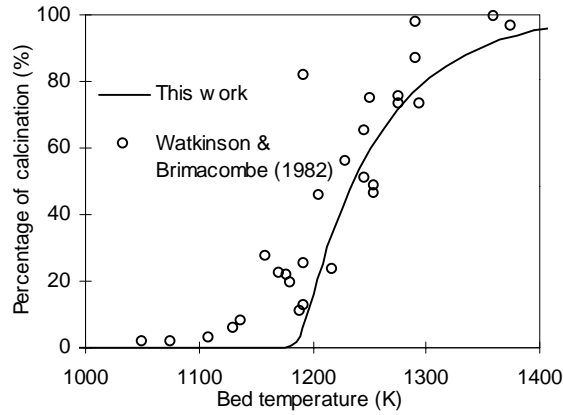
Figure 5 – Percentage of limestome calcination.

The data measured by Watkinson & Brimacombe (1982) are also shown. The predicted values were in good agreement with the measured ones, with a maximum percentage difference smaller than 10%. The average percentage calcination measured by Watkinson & Brimacombe (1982) at the discharge end of the kiln was 97.6%. In the present work, the predicted value was 99.02% (relative difference of –1.45%). Watkinson & Brimacombe (1982) observed that the bed height varied in the axial direction from 47mm at the limestone charge end to 92mm at the discharge end of the kiln. This variation in bed height corresponds to a variation in the local degree of fill of 6.5 to 17%, respectively, and it causes the bed axial velocity to decrease from the charge to the discharge end of the kiln. The predicted axial velocity profile for the bed is presented in Fig. 6.
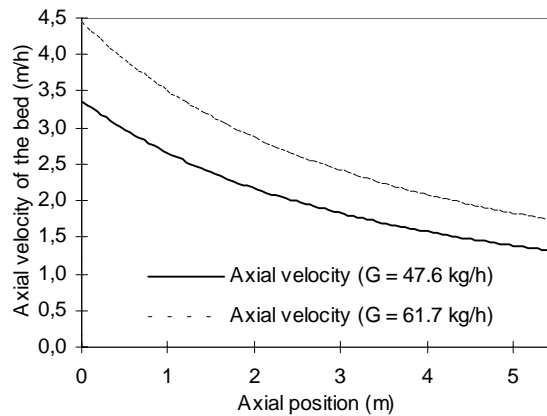

Figure 6 – Axial velocity profile for limestome bed.

These velocity profiles were used in the calculation of the particles residence time in the kiln. The calculated value was 2.77h for the limestone feed rate of 47.6 kg/h. This predicted value is within the range measured by Watkinson & Brimacombe (1982): 3.0h for a feed rate of 48.6 kg/h, and 2.2h for a feed rate of 46.7 kg/h.

5. CONCLUSIONS

A steady-state one-dimensional model was developed to describe limestone calcination in a rotary kiln. The model provides a description of the calcination reaction kinetics, the heat and mass transfer phenomena between the solid bed and the gas phase, and the rheology of the bed. Simulation results allowed a detailed evaluation of the effects of changes in the operational variables on the performance of the kiln and on the final quality of the product. The results presented good agreement with experimental data reported in the literature.

REFERENCES

Barr, P.V., Brimacombe, J.K. & Watkinson, A.P. ,1989, A Heat Transfer Model for the Rotary Kiln: Part I. Pilot Kiln Trials. Metall. Trans. B, vol. 20B, pp. 391-402.

Brooks, D.G. ,1989, Mathematical Simulation of a Rotatory Coke Calciner. Light Met. Proc. Tech. Sess. AIME 118th Annual Meeting, pp. 461-469.

Davis, R.A. ,1996, Mathematical Model of Magnetite Oxidation in a Rotary Kiln Furnace, Can. J. Chem. Eng., vol. 34, pp. 1004-1009.

Gordon, R.A. ,1969, Steady-State Model of a Carbon Kiln Developed for Alcan, Canadian General Eletric Report, Arvida, Canada.

Henein, H., Brimacombe, J.K. and Watkinson, A.P. ,1983, Experimental Study of Transverse Bed Motion in Rotary Kilns, Metall. Trans. B, vol. 14B, 191-206.

Hills, A.W.D. ,1968, The Mechanism of the Thermal Decomposition of Calcium Carbonate, Chem. Eng. Sci., vol. 23, pp. 297-320.

Hottel, H.C. & Sarofim, A.F. ,1967,. Radiative Transfer ,1st Edition, McGraw-Hill Inc., New York, USA.

Ketlakh, G.A. & Tsibin, I.P. ,1978, Heat Transfer by radiation in Rotary Kiln, translated from Ogneupory, vol. 1, pp. 17-19.

Li, K.W. & Friday, J.R. ,1974, Simulation of Coke Calciners, Carbon, vol. 12, pp. 225-231.

Martins, M.A. and Oliveira, L.S. ,1998, Modelagem e Simulação de Fornos Rotativos para Calcinação de Coque de Petróleo, Proc. XVI Congresso Brasileiro de Sistemas Particulados, vol. 2, pp. 509-516, Teresópolis, Brazil (Portuguese).

Martins, M.A. ,1999, Modelagem e Simulação de Sistemas de Calcinação, M.Sc. Thesis, Universidade Federal de Minas Gerais, Belo Horizonte, Brazil. (Portuguese).

Özisik, M.N. ,1985, Heat Transfer ,2nd ed., McGraw-Hill Inc., Montreal, CA.

Perron, J. & Bui, R.T. ,1990, Rotary Cylinder: Solid Transport Prediction by Dimensional and Rheological Analysis, Can. J. Chem. Eng., vol. 68, pp. 61-68.

Perron, J. Bui, R.T. & Nguyen, H.T. ,1992, Modélisation d'un Four de Calcination du Coke de Pétrole: I. Le Modèle, Can. J. Chem. Eng., vol. 70, pp. 1108-1119.

Pitts, D.R. & Sissom, L.E. ,1991, 1000 Solved Problems in Heat Transfer - Schaum's Solved Problems Series ,1st ed., McGraw-Hill Inc., New York, USA.

Reddy, J.N. & Gartling, D.K. ,1994, The Finite Element Method in Heat Transfer and Fluid Dynamics ,1st ed., CRC Press Inc., Boca Raton, USA.

Sood, R.R., Clark, R. & Stokes, D.M. ,1972, Computerized Model in Determine and Operating Parameter for Rotatory Kilns for Petroleum Coke Calcination, Light Met. Proc. Tech. Sess. AIME 101st Annual Meeting, pp. 151-161.

Tscheng, S.H. & Watkinson, A.P. ,1979, Convective Heat Transfer in a Rotary Kiln, Can. J. Chem. Eng., vol. 57, pp. 433-443.

Watkinson, A.P. and Brimacombe, J.K. ,1982, Limestone Calcination in a Rotary Kiln, Metallurgical Transactions B, vol. 13B, pp. 369-378.